Inorg. Chem. **2004**, *43*, 3210–3218

Crystallographic, Electronic, and Magnetic Studies of ζ_2-GaM (M = Cr, Mn or Fe): Trends in Itinerant Magnetism

Olivier Gourdon,[†] Sergey L. Bud'ko,[‡] Darrick Williams,[§] and Gordon J. Miller*[,†]

Department of Chemistry and Ames Laboratory, U.S. Department of Energy, Iowa State University, Ames, Iowa 50011-3111, Department of Physics and Ames Laboratory, U.S. Department of Energy, Iowa State University, Ames, Iowa 50011-3111, and Los Alamos National Laboratory, Los Alamos, New Mexico 87545

Received December 10, 2003

This study of the crystal structure, electronic structure, and magnetic properties of the ζ_2-GaM (M = Cr, Mn or Fe) alloys is motivated by the recent reinvestigation of the crystallographic Al_8Cr_5 structure type of ζ_2-GaMn. The isostructural compounds ζ_2-GaFe and ζ_2-GaCr have been refined using X-ray powder diffraction as well as neutron powder diffraction for ζ_2-GaFe. Their structures have been refined using the space group $R\bar{3}m$, with cell parameters $a = 12.625(8)$ Å and $c = 7.785(10)$ Å for ζ_2-GaCr and $a = 12.4368(11)$ Å and $c = 7.7642(10)$ Å for ζ_2-GaFe. Band structure calculations using the self-consistent, spin-polarized TB-LMTO method were performed to understand their electronic structure and magnetic properties. Band calculations show that from GaCr to GaFe the magnetic interactions change from weakly antiferromagnetic coupling to ferromagnetic coupling. Magnetic measurements confirm ferromagnetism for GaFe and show a weak paramagnetic response for GaCr.

Introduction

During our recent exploration of new approximants to quasicrystals in Ga−Mn systems, we reinvestigated the crystal structure and the physical properties of the ζ_2-GaMn phase,[1] which was discovered in the 1960s.[2,3] ζ_2-GaMn was assigned to the Al_8Cr_5 structure type (space group $R3m$) from X-ray powder diffraction, but our work showed the centrosymmetric space group $R\bar{3}m$, with $a = 12.605(2)$ Å and $c = 8.0424(11)$ Å, to be more accurate. Moreover, the atomic positions and displacement parameters, which were missing in the previous study, are now refined. Motivated by our work on the ζ_2-GaMn structure and the possibility of interesting magnetic properties, we have performed similar investigations on GaFe and GaCr. Indeed, previous studies showed that GaFe and GaCr binary alloys may also adopt the Al_8Cr_5 structure type.[3,4]

The crystal structure of these compounds is quite interesting since it adopts a complex atomic network of icosahedra and dodecahedra, whereas the formula unit GaM is relatively simple. To our knowledge, there are no such complex structures in other binary systems for a 1:1 composition. The stability of this structure versus a NaCl structure type or a CsCl structure type, for example, brings some questions about the close relation between atomic structure and electronic structure. The relative complexity of the atomic structure and the presence of icosahedra and dodecahedra highlight the quasicrystal approximant character of this phase. Indeed, it is generally believed that quasicrystals are built up by large "clusters" arranged aperiodically. By "clusters" we mean structural units based on the assemblage of certain polyhedra such as dodecahedra and icosahedra as observed in ζ_2-GaM as well as in Ga_6Mn_5 and $Ga_{137}Mn_{124}$. In these phases, which are close in composition to ζ_2-GaMn, we observe a different periodic arrangement of the dodecahedral and icosahedral "clusters". All approximant phases in the Ga−Mn system exist in a composition range from 49 at. % to 62 at. % Ga.[5] Further information concerning a "cluster" description may be found in ref 1. The Ga−Mn system has been recently reinvestigated by Boström et al.[5] Numerous

* To whom correspondence should be addressed. E-mail: gmiller@iastate.edu.
[†] Department of Chemistry and Ames Laboratory, U.S. Department of Energy, Iowa State University.
[‡] Department of Physics and Ames Laboratory, U.S. Department of Energy, Iowa State University.
[§] Los Alamos National Laboratory.

(1) Gourdon, O.; Miller, G. J. *J. Solid State Chem.* **2003**, *173*−*1*, 137−147.
(2) Schubert, K.; Anantharaman, T. R.; Ata, H. O. K.; Meissner, H. G.; Pötzschke, M.; Rossteutscher, W.; Stolz, E. *Naturwissenschaften* **1960**, *47*, 512.
(3) Meissner, H. G.; Schubert, K. *Z. Metallkd.* **1965**, *56*, 523.
(4) Bornand, J. D.; Feschotte, P. *J. Less-Common Met.* **1972**, *29* (1), 81−91.
(5) Boström, M. Doctoral Dissertation, Stockholm University, Sweden, 2002.

10.1021/ic035419f CCC: $27.50
Published on Web 04/10/2004

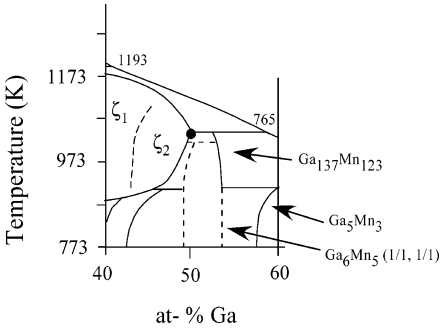

Figure 1. Representation of the Ga−Mn binary phase diagram in the atomic range 40−60% of Ga.

phases are present in that system, as well as in the Ga−Fe and Ga−Cr systems, and the selected synthesis of a single phase, like the ζ_2 phase, is sometimes quite a challenge. For example, Figure 1 presents schematically the Ga−Mn phase diagram at high temperature (over 500 °C) in the composition range 40−60 in atomic percentage in Ga, which is based on the work done by Boström.[5] This scheme shows the difficulty to synthesize the ζ_2 phase as a pure phase. This phase is stable within a short temperature range, from 650 to 850 °C. Moreover, numerous phases surround the ζ_2 phase, such as the cubic ζ_1 phase (at ca. 40 atomic percent Ga), Ga_6Mn_5, $Mn_{123}Ga_{137}$, and Mn_3Ga_5.[5] Thus, from the liquidus, $Mn_{123}Ga_{137}$ is easier to precipitate than the ζ_2 phase and it may explain why its atomic structure has never been refined before, although the composition is quite simple. Notice that, from Boström,[5] the ζ_2 phase is stable in a small range of composition from approximately 45 at. % Ga to 50 at. % Ga. However, our interest was only the study of the upper limit of this range, and the compositions of our samples have been verified by numerous analyses (EDXS, X-ray refinement, and neutron refinement).

The ζ_2-GaM structure is a good example to investigate the evolution of itinerant magnetic properties since we find that this structure exists for M = Cr, Mn, and Fe. Indeed, these three elements themselves are especially interesting for their intrinsic magnetic properties. However, it is somewhat complicated to compare them directly because they adopt different structure types. Indeed, both Cr and Fe adopt a bcc structure type whereas α-Mn is a complex, body-centered structure formed by Mn_{12} icosahedra. In this work, we examine the evolution of electronic and magnetic structure from Cr to Fe in an identical atomic arrangement obtained in the ζ_2-GaM structure type. A similar study combining theory and synthesis in a series of iron/manganese rhodium borides was performed by R. Dronskowski et al.[6] On the basis of the same structure type for both the iron and the manganese compounds, they investigated and elucidated their magnetic properties by studying the nature of the M−M bonding interactions in these boride compounds.

Experimental Section

General Synthesis. GaFe and GaCr samples were obtained from equal molar mixtures of the corresponding elements [Ga (99.999%, Aldrich), Cr powder (99.99%, Johnson), and Fe powder (99.99%, Alfa)]. The Cr and Fe powders were treated first by heating them in an arc welder furnace. The mixture of treated transition metal and gallium was placed in a sealed, evacuated silica tube at 1023 K for 4 days. After slow cooling (30 h) to 723 K, the closed furnace was turned off and cooled naturally to room temperature. The products appear to be air- and moisture-stable over a period of several months and stable in diluted acid. The samples were examined by electron microprobe (JEOL 840A) and found to be free of other elements. Analysis by energy-dispersive X-ray spectroscopy gave the average chemical compositions $Ga_{0.51(1)}Cr_{0.49(1)}$ and $Ga_{0.51(1)}Fe_{0.49(1)}$. To obtain the quantitative values, GaAs, Cr_2O_3, and Fe_2O_3 were used as standards.

Table 1. Structural Data and Crystallographic Data Recording/ Refinement Conditions for ζ_2-GaCr

composition	$Ga_{13}Cr_{13}$
space group	$R\bar{3}m$ (*hR*26)
cell params	$a = 12.625(8)$ Å
	$c = 7.785(10)$ Å
V (Å^3)	1074.6
Z	3
D (calcd, g cm^{-3})	7.323
X-ray machine	Scintag XDS-2000 diffractometer
wavelength	Cu Kα_1 and Cu Kα_2
2θ, step	20°−80°, 0.01°
reflns	216
fitted params	26
refinement, program	Rietveld, Jana2000
$R_I = \sum\|I_o - I_c\|/\sum\|I_o\|$	0.028
$R_p = \sum\|y_{oi} - y_{ci}\|/\sum\|y_{oi}\|$	0.032
$R_{wp} = (\sum w_i(y_{oi} - y_{ci})^2/\sum w_i(y_{oi})^2)^{1/2}$ [a]	0.055

[a] $w_i = (y_{oi})^{-1/2}$.

Table 2. Fractional Atomic Coordinates and Equivalent Isotropic Displacement Parameters[a] (Å^2) for ζ_2-GaCr

	x	y	z	B_{eq}
Ga1	0	0	0	0.92(6)
Ga2	0.2346(10)	0.1173	0.5765(3)	1.23(5)
Ga3	0.2893(10)	0.2893	1/2	1.02(5)
Cr1	0	0	1/2	0.86(8)
Cr2	0.23722(14)	0.11861	0.9287(3)	0.94(7)
Cr3	−0.14840(14)	−0.07420	0.7532(3)	0.78(6)

[a] $B_{eq} = (8\pi^2/3)\sum_i\sum_j\sum_{ij}a_i^* a_j^* \mathbf{a}_i\mathbf{a}_j$.

Crystal Structure Determination. Powder Diffraction Study of ζ_2-GaCr and ζ_2-GaFe. X-ray Studies. The X-ray powder diffraction patterns of these two phases were recorded on a Scintag XDS-2000 $\theta-\theta$ powder diffractometer mounted on a sealed tube generator with a Cu target. The structures of ζ_2-GaCr and ζ_2-GaFe had not been refined prior to the present study, although the cell parameters were determined from X-ray powder diffraction diagrams.[3,4] On the basis of the structural arrangement of ζ_2-GaMn, the cell parameters and the atomic positions of ζ_2-GaCr and ζ_2-GaFe were successfully refined with the Rietveld method, using the Jana2000 program.[7] This confirms the symmetry, space group, and cell parameters of these two phases, and no evidence of superstructures has been observed. Tables 1−4 summarize the data collection parameters and the refinement results along with the atomic positions. Figure 2 gives the observed and calculated diagrams along with the difference curves for ζ_2-GaCr and ζ_2-GaFe.

Neutron Studies. Since the scattering factors for Ga and Fe may be difficult to discern by X-ray powder diffraction, neutron powder diffraction was attempted on ζ_2-GaFe. Time of flight (TOF) neutron diffraction data were collected at the Manuel Lujan Neutron Science

(6) Dronskowski, R.; Korczak, K.; Lueken, H.; Jung, W. *Angew. Chem., Int. Ed.* **2002**, *41* (14), 2528−2532.

(7) Petricek, V.; Dusek, M. *The crystallographic computing system JANA2000*; Institute of Physics: Praha, Czech Republic, 2000.

Table 3. Structural Data and Crystallographic Data Recording/ Refinement Conditions for ζ_2-GaFe

composition	$Ga_{13}Fe_{13}$
space group	$R\bar{3}m$ (*hR*26)
cell params	$a = 12.4368(11)$ Å [12.4218(11) Å]
	$c = 7.7642(10)$ Å [7.7576(11) Å]
V (Å^3)	1040.0
Z	3
D (calcd, g cm^{-3})	7.816
X-ray machine	Scintag XDS-2000 diffractometer
wavelength	Cu Kα_1 and Cu Kα_2
2θ, step	20°−80°, 0.01°
reflns	212
fitted params	26
refinement, program	Rietveld, Jana2000
$R_I = \sum\|I_o - I_c\|/\sum\|I_o\|$	0.035
$R_p = \sum\|y_{oi} - y_{ci}\|/\sum\|y_{oi}\|$	0.050
$R_{wp} = (\sum w_i(y_{oi} - y_{ci})^2/\sum w_i(y_{oi})^2)^{1/2}$ [a]	0.063

[a] $w_i = (y_{oi})^{-1/2}$.

Table 4. Fractional Atomic Coordinates and Equivalent Isotropic Displacement Parameters[a] (Å^2) for ζ_2-GaFe[b]

	x	y	z	B_{eq}
Ga1	0	0	0	1.50(7)
	0	0	0	1.59(7)
Ga2	0.2366(7)	0.1183	0.5727(8)	1.15(4)
	0.2336(3)	0.1168	0.5739(4)	1.54(3)
Ga3	0.2805(6)	−0.0529(6)	5/6	0.97(4)
	0.2796(3)	−0.0537(3)	5/6	0.86(2)
Fe1	0	0	1/2	0.66(6)
	0	0	1/2	0.63(4)
Fe2	0.2310(8)	0.1155	0.9254(9)	0.68(5)
	0.2328(2)	0.1164	0.9218(2)	0.80(2)
Fe3	−0.1412(8)	−0.0706	0.7493(10)	0.71(5)
	−0.1447(2)	−0.07233	0.7483(4)	0.77(2)

[a] $B_{eq} = (8\pi^2/3)\sum_i\sum_j\sum_{ij} a_i^* a_j^* \mathbf{a}_i\mathbf{a}_j$. [b] In italics are listed the parameters refined by neutron diffraction.

Center located at Los Alamos National Science Center (LANSCE) on the high-pressure preferred orientation (HIPPO) powder diffractometer. The instrument utilizes chilled water as a moderator and has short primary flight path distance (moderator to sample) of 10 m for the sake of higher neutron flux at the expense of resolution. The data were collected at 300 K using the 140°, 90°, and 40° detector banks, in which each group of detector banks was individually refined (8 detector banks for 140°, 10 for 90°, and 12 for 40°) following the collection, and covers a *d* spacing range from 0.4 to 13.9 Å for HIPPO. Data for all 30 detectors banks refined comparably, and the results reported below are for the collective sum of the 8 individual histograms of the 140° detector banks and the 12 individual histograms of the 40° detector banks.

The structure was refined using the General Structure Analysis System (GSAS), a Rietveld profile analysis program developed by Larson and Von Dreele.[8] The starting structural model used was from the single-crystal X-ray data. The structural model was refined for unit cell parameters, atomic positions, and isotropic thermal parameters. Background coefficients, scale factors, isotropic strain terms in the profile function, and sample absorption were also refined for a total of 144 parameters for the 140° and 40° detector banks. The fit confirms the assignment of the Ga and Fe atomic sites from X-ray diffraction. The final refinement corresponds to χ_2 value of 1.97 for the summation of the individual histograms 140° and 40° detector banks (wRp = 4.4%). When the occupancies were allowed to refine, they settled around 1, indicating no mixed Ga/Fe sites in the compound. Figure 3 illustrates the observed and

(8) Larson, A. C.; Von Dreele, R. B. *GSAS: General Structure Analysis System*; 1985.

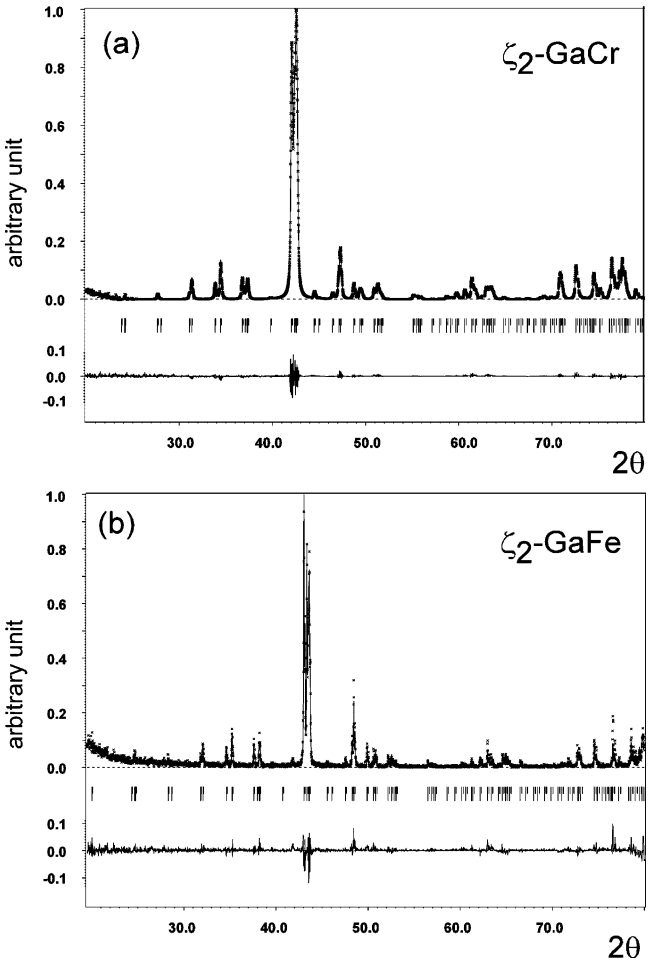

Figure 2. X-ray powder diffraction patterns observed and calculated of ζ_2-GaCr and ζ_2-GaFe. The difference is illustrated on the same scale.

calculated diagrams obtained by neutron diffraction on ζ_2-GaFe. The cell parameters and the atomic positions are listed in Tables 3 and 4 in italics.

Figure 4a shows the rhombohedral ζ_2-GaM (M = Cr, Mn, Fe) crystal structure along the *c* axis. This structure can be described easily and is based upon icosahedra and dodecahedra shown in Figure 4b,c. Icosahedra (Figure 4b) of 12 M atoms surround Ga sites at (0, 0, 0), ($^2/_3$, $^1/_3$, $^1/_3$), and ($^1/_3$, $^2/_3$, $^2/_3$). These icosahedra are surrounded by dodecahedra (Figure 4c) of 18 Ga atoms and 2 M atoms. The dodecahedra are interconnected by Ga edges and isolated M atoms. From the magnetic point of view, we can describe this structure by a 1D magnetic structure model along the *c* axis with a regular succession of M_{12} icosahedra bridged together by isolated M atoms as presented in Figure 4d. These chains, located along (0, 0, *z*), ($^2/_3$, $^1/_3$, *z*), and ($^1/_3$, $^2/_3$, *z*), are separated from one another by a network of Ga atoms.

Susceptibility Measurements. Temperature and magnetic field dependent dc magnetization measurements in the ranges of the parameters 1.8−300 K and 0−55 kOe were carried out using a Quantum Design, Inc., MPMS-5 SQUID magnetometer. Magnetic measurements have been carried out on bulk samples (approximately 200 mg) from the same preparations as the ones used for powder diffraction experiments.

Figure 5a,c shows field dependent magnetization data taken at 5 K for ζ_2-GaCr and ζ_2-GaFe, respectively. While the *M*(H) curve for ζ_2-GaCr is practically linear and the magnetization value *M*(5 K, 55 kOe) is only slightly above 1.2 emu/mol, the field dependent

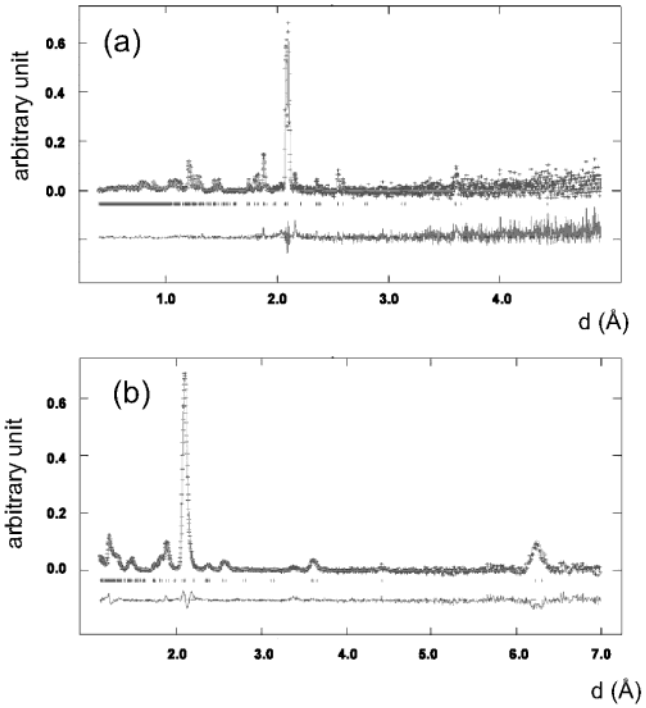

Figure 3. Time of flight (TOF) neutron powder diffraction patterns observed and calculated of ζ_2-GaFe. The measurement have be carried out at $\theta = 3.2°$. The Rietveld refinement of neutron powder diffraction data for GaFe. Part a represents 1 of the 8 individual histogram of the 140° detector banks and part b represents 1 of the 12 individual histogram of the 40° detector banks. The upper curve is the experimental data, and the lower is (experiment-calculated) on the same scale.

magnetization for ζ_2-GaFe is nonlinear with a clear trend to saturation and almost 3 orders of magnitude higher M(5 K, 55 kOe) value than for ζ_2-GaCr.

Temperature dependent susceptibilities for each compound (taken in 1 kOe applied magnetic field) confirm the significant difference in magnetic behavior of the two compounds. The susceptibility of ζ_2-GaCr (Figure 5b) is basically temperature independent ($\sim 2.4 \times 10^{-4}$ emu/mol) with small Curie-like upturn at low temperature, which possibly originates from a small amount of some paramagnetic impurities. A small feature of currently unknown origin is observed for this material at about 165 K. The temperature dependent susceptibility of ζ_2-GaFe (Figure 5d) is much higher (0.02−0.07 emu/mol below 300 K) and has two distinct features: a peak at $\sim$ 42 K possibly associated with a magnetic transition and a broad maximum at $\sim$135 K. Susceptibility decreases with an increase of temperature between 200 and 300 K in a Curie−Weiss-like manner.

The general magnetization behavior observed for each compound is in qualitative agreement throughout samples from different batches with the observed differences being due to small amounts of possible secondary phases that often may give considerable contribution to magnetization.

The following summarizes the magnetic measurements: While the exact ground state of each compound requires further, detailed macroscopic and microscopic measurements and possibly further improvement in sample quality, our data are consistent with much stronger magnetic interactions in ζ_2-GaFe with a possibility of ferromagnetism, while magnetic interactions in ζ_2-GaCr appear to be much weaker and the compound possibly is nonmagnetic or weakly antiferromagnetic as seen in other Ga−Cr binary phases such as Ga_6Cr_5 or Ga_5Cr_3.[9]

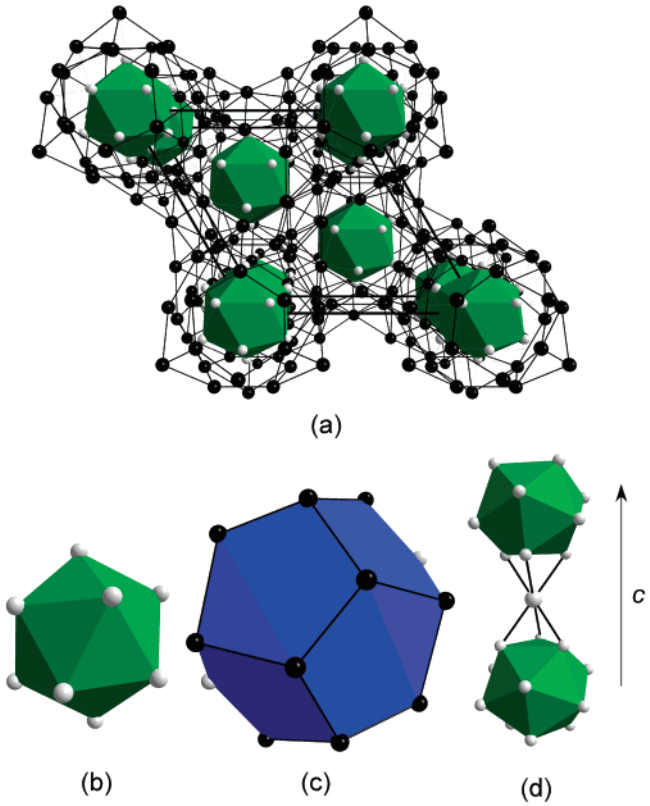

Figure 4. The GaMn structure emphasizing various cluster units: (a) unit cell along the *c* axis showing the icosahedra mostly surrounded by Ga atoms; (b) icosahedra of Mn around a Ga site; (c) dodecahedra of 18 Ga sites and 2 Mn sites; (d) connection between two icosahedra via the Mn site on the dodecahedra. The gray and black spheres represent the Mn atoms and Ga atoms, respectively.

Electronic Structure Calculations

During our reinvestigation of the ζ_2-GaMn phase, spin-polarized calculations were performed to understand the possible magnetic behavior of this compound. A similar effort on ζ_2-GaCr and ζ_2-GaFe is presented here to explain the magnetic behavior of these isostructural compounds.

Computational Details. Tight-binding, linear muffin-tin orbital (TB-LMTO) electronic band structure calculations were carried out in the atomic sphere approximation using the LMTO47 program.[10−13] Exchange and correlation were treated in a local spin density approximation.[14] All relativistic effects except spin−orbit coupling were taken into account using a scalar relativistic approximation.[15]

In the atomic sphere approximation, space is filled with small overlapping Wigner−Seitz (WS) atomic spheres. The symmetry of the potential is considered spherical inside each WS sphere, and a combined correction is used to take into account the overlapping part.[16] The radii of the WS spheres

(9) Booth, J. G.; Mankikar, R. M.; Morris, P. G. *Solid State Commun.* **1986**, *60* (1), 1−2.
(10) Andersen, O. K. *Phys. Rev. B* **1975**, *12*, 3060−3083.
(11) Andersen, O. K.; Jepsen, O. *Phys. Rev. Lett.* **1984**, *53*, 2571−2574.
(12) Andersen, O. K.; Jepsen, O.; Glötzel, D. In *Highlights of condensed-matter theory*; Bassani, F., Fumi, F., Tosi, M. P., Eds.; North-Holland: New York, Lambrecht, W. R. L., 1985.
(13) Andersen, O. K. *Phys. Rev. B* **1986**, *34*, 2439−2449.
(14) von Barth, U.; Hedin, L. *J. Phys. C* **1972**, *5*, 1629−1642.
(15) Koelling, D. D.; Harmon, B. N. *J. Phys. C* **1977**, *10*, 3107−3114.
(16) Jepsen, O.; Andersen, O. K. *Z. Phys. B* **1995**, *97*, 35−47.

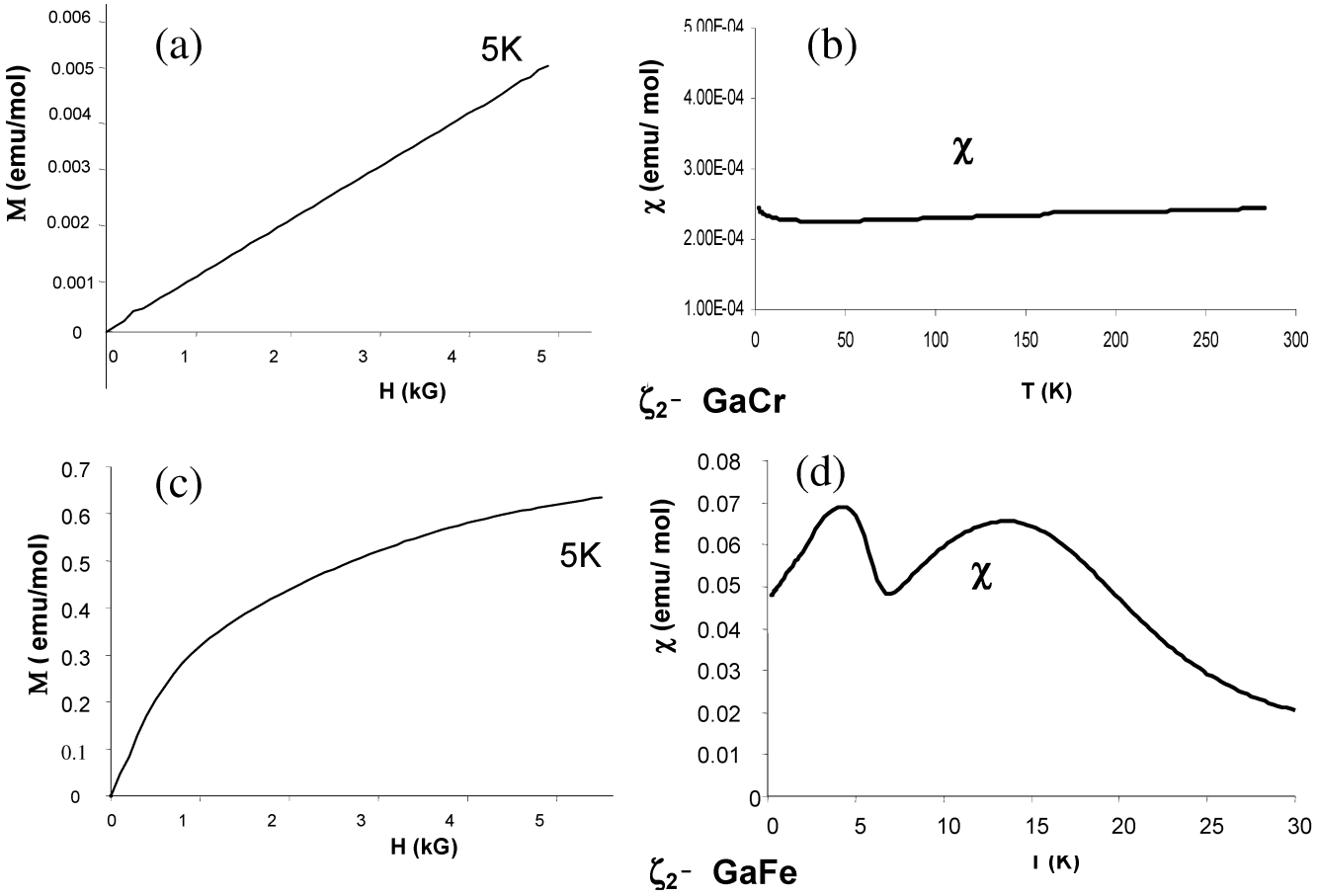

Figure 5. Magnetization data taken at 5 K for (a) ζ_2-GaCr and (c) ζ_2-GaFe and susceptibility data for (b) ζ_2-GaCr and (d) ζ_2-GaFe in the temperature range 1.8−300 K.

were obtained by requiring that the overlapping potential be the best possible approximation to the full potential, and were determined by an automatic procedure.[16] This overlap should not be too large because the error in the kinetic energy introduced by the combined correction is proportional to the fourth power of the relative sphere overlap. Interatomic space was filled with one interstitial sphere since the structure of the compound under examination is not densely packed. The optimal position and radius (r_{ES}) of this "empty sphere" (ES) was determined according to the method described in ref 13. The WS radii of M (M= Cr, Mn, Fe) and Ga atoms are nearly equal ($1.47 < r_M < 1.48$ Å and $1.45 < r_{Ga} < 1.46$ Å), while the empty sphere has a radius of 0.78 Å and is located on the pentagonal faces of the dodecahedra.

The basis set included Ga 4s, 4p, and 4d orbitals and M 4s, 4p, and 3d orbitals. For the ES only s and p orbitals were used. The Ga 4d orbital and the ES p orbital were treated by the Löwdin downfolding technique.[10−13] The *k*-space integrations were performed by the tetrahedron method.[17] The self-consistent charge density was obtained using 64 irreducible *k*-points in the Brillouin zone for the rhombohedral cell. The contribution of the nonspherical part of the charge density to the potential was neglected. Both non-spin-polarized and spin-polarized calculations were performed. The Fermi level was selected as the energy reference.

(17) Blöchl, P. E.; Jepsen, O.; Andersen, O. K. *Phys. Rev. B* **1994**, *49*, 16223−16233.

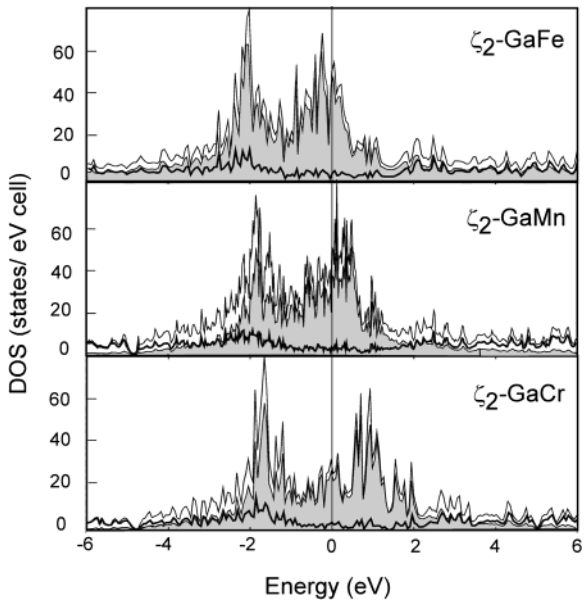

Figure 6. Total density of states (TDOS) and different partial densities of states (PDOS) for the non-spin-polarized calculations on ζ_2-GaM (M = Cr, Mn, Fe).

Nonmagnetic ζ_2-GaM (M = Cr, Mn, Fe). In Figure 6 the total densities of states (TDOS) and different partial densities of states (PDOS) for the non-spin-polarized calculations on the ζ_2-GaM (M = Cr, Mn, Fe) structure are presented (PM). The PDOS of the M-3d (M = Cr, Mn, Fe)

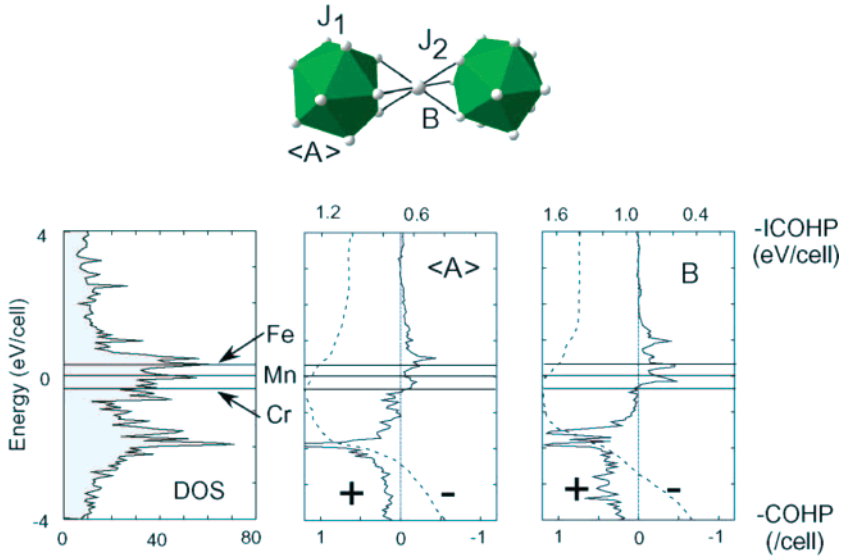

Figure 7. TDOS and M−M COHP curves for the ζ_2-GaM (M = Cr, Mn, Fe) compounds.

orbitals are shaded in gray whereas the 4p orbitals are represented by a thick line. The profile of the TDOS is close to the PDOS of the M-3d functions, which suggests that the icosahedra dominate the electronic properties.

The shape of the TDOS in the vicinity of the Fermi level corresponds mostly to two broad peaks: one centered around −2 eV and the second one below (ζ_2-GaFe), centered on (ζ_2-GaMn), or above (ζ_2-GaCr) the Fermi level depending on the nature of the transition metal M. The Ga 4p PDOS is relatively flat with the highest density around −2 eV. So, a small interaction is expected between the Ga 4p orbitals and M 3d orbitals. Integration of the M 3d PDOS shows that approximately 50% (ζ_2-GaCr), 60% (ζ_2-GaMn), and 70% (ζ_2−GaFe) of the 3d states are occupied. The three TDOS curves suggest that a rigid band model holds reasonably well for ζ_2-GaM (M = Cr, Mn, Fe). The primary distinctive feature is a narrowing of the two-peak feature. The M orbitals from the icosahedral sites and the dodecahedral sites have been plotted together. However, our previous study on ζ_2-GaMn has shown a slight difference in the PDOS due to the local environment.[1] The environment of the M atoms from the dodecahedral sites, presented in Figure 4d, is trigonal antiprismatic with six rather short M−M distances (B) (∼2.5 Å). Consequently, we treat the M−M interactions separately using a COHP (crystal overlap Hamilton population[18]) analysis ($\langle A \rangle$ represents the average M−M distance in the icosahedron).These COHP curves, as well as the TDOS for ζ_2-GaMn, are presented in Figure 7 as representative of the entire series. In this and subsequent figures the icosahedra are shown as circles. Indeed, the first peak at −2 eV corresponds to M−M bonding interactions, whereas the second one close to the Fermi level corresponds to M−M antibonding states. In ζ_2-GaCr, the highest populated states are M−M nonbonding. Indeed, the Fermi level corresponds perfectly to the crossing between the bonding and the antibonding states among M−M interactions. The situation is different for ζ_2-GaMn and ζ_2-GaFe, since antibonding states are populated. However, according to Figure 7, the Fermi level for ζ_2-GaMn corresponds to a deep minimum in these antibonding states, close to nonbonding, especially for the Mn−Mn interactions inside the icosahedra, whereas for ζ_2-GaFe the antibonding states are more pronounced.

To summarize, calculations without spin polarization show that the DOS at the Fermi level is very high (between 30 and 60 states/eV/cell). A progression in the bonding character of these states is also observed. Indeed, these states have M−M nonbonding character for ζ_2-GaCr, while there is M−M antibonding character for ζ_2-GaFe (Figure 7). For ζ_2-GaMn, the situation lies between both cases (nonbonding/antibonding states). Dronskowski et al. have already shown that a driving force for antiferromagnetism or ferromagnetism lies in the local nonbonding or antibonding character of the states around the Fermi level.[19] Consequently, according to the Stoner criteria[20] and on the basis of our previous work on ζ_2-GaMn, magnetic properties may also be expected for ζ_2-GaCr and ζ_2-GaFe, and spin-polarized calculations should be performed to understand their electronic structures. Indeed, Stoner presented in 1938 a predictive model of itinerant-electron ferromagnetism by assuming an average spin field interacting with a single spin. The Stoner criterion can be expressed as

$$I \times \mathrm{DOS}(\epsilon_F) > 1$$

where I is a measure of the strength of the exchange interaction in the metal and DOS(ϵ_F) is the density of states at the Fermi level, ϵ_F. Nowadays, most solid-state physicists consider the Stoner criterion as a good indicator of whether a metal or an alloy will be ferromagnetic. The DOS(ϵ_F) value is directly accessible by band structure calculations, and I values may be found in various papers. The first tabulation

(18) Hughbanks, T.; Hoffmann, R. *J. Am. Chem. Soc.* **1983**, *105*, 3528−3537.

(19) Landrum, G. A.; Dronskowski, R. *Angew. Chem., Int. Ed.* **2000**, *39*, 1560−1585.

(20) Stoner, E. C. *Proc. R. Soc. London* **1938**, *165*, 372−387.

Table 5. Results of Spin-Polarized Band Structure Calculations Obtained for ζ_2-GaCr, ζ_2-GaMn, and ζ_2-GaFe

		M = Mn		
	M = Cr	FM1	FM2	M = Fe
Ga1 (μB)	−0.004	−0.085	−0.039	−0.058
Ga2 (μB)	0.022	−0.048	0.030	−0.058
Ga3 (μB)	0.024	−0.064	0.053	−0.076
M1 (μB)	−0.699	−1.979	1.837	2.100
M2 (μB)	−0.791	2.096	−1.968	1.686
M3 (μB)	1.279	2.576	2.352	2.193
Total (μB/cell)	2.529	25.243	4.641	24.442
ΔE (eV/cell) (relative to the paramagnetic calculation)	−0.067	−1.69	−1.45	−2.71

was created by Janak in 1977[21] and gives I values for Cr (bcc), Mn (fcc), and Fe (bcc) as 0.38, 0.41, and 0.46 eV, respectively. Therefore, the Stoner criteria for ζ_2-GaM, M = Cr, Mn, and Fe are 0.71, 0.98, and 1.60 per M atom. These values for the Stoner criteria are only a first approximation because I values for each atom are dependent upon the local environment.[21] Rigorously, I values should have been calculated for each of the three M crystallographic sites (M = Cr, Mn, or Fe) since their local environments are different. Moreover, for these binary alloys of Ga, even if magnetic properties are not expected for Ga, the Ga PDOS at the Fermi level may affect the Stoner criterion value. Anyway, from these approximate values we may expect ferromagnetism for ζ_2-GaFe and possibly ζ_2-GaMn. However, the Mn case seems to be a critical one, as already observed,[1] since the value for the Stoner criterion is rather close to 1.

Spin-Polarized Calculations on ζ_2-GaM (M = Cr, Mn, Fe). Different initial magnetic models were attempted that retained the 3-fold symmetry axis, but only two models converged (FM1 and FM2) for ζ_2-GaMn, both of which retain a centrosymmetric potential.[1] For ζ_2-GaCr and ζ_2-GaFe, identical models were examined, but just one magnetic model was found more stable than the nonmagnetic one for each compound. The final results for the spin-polarized calculations are listed in Table 5. We will briefly summarize the results obtained on ζ_2-GaMn before discussing ζ_2-GaCr and ζ_2-GaFe.

Considering only the M sites, which dominate the magnetic behavior, the ζ_2-GaM structure can be described as a 1D magnetic compound. Indeed, along the c axis we observe a regular succession of icosahedra and isolated M atoms bridging these icosahedra. Consequently, we can consider two different couplings: a J_1 coupling between M atoms within icosahedra (M(ico)−M(ico)) and a J_2 coupling between the icosahedron and the bridging atom (M(ico)−M(dodeca)). The majority (spin-up) direction is indicated by ↑ and the minority (spin-down) direction by ↓.

ζ_2-GaMn. The two magnetic models FM1 and FM2 correspond to two different Mn−Mn coupling arrangements. In FM1 the Mn−Mn J_1 couplings are ferromagnetic whereas the Mn−Mn J_2 coupling is antiferromagnetic. In FM2, these couplings are opposite. Both models are very close in energy, differing by just 0.24 eV/formula unit.

ζ_2-GaCr and ζ_2-GaFe. For each of these compounds only one magnetic model has been found to be more stable than the nonmagnetic one. These models confirm the hypothesis of antiferromagnetism and ferromagnetism already discussed for ζ_2-GaCr and ζ_2-GaFe, respectively. The atomic magnetic moments are listed in Table 5. In the chromium compound both the J_1 and J_2 couplings are antiferromagnetic whereas they are ferromagnetic in the iron compound. However, the total energy difference between the magnetic and the nonmagnetic models increases from Cr to Fe. Moreover, the atomic magnetic moments are rather low on the Cr atoms (∼0.8 μB) compared to those on the Fe atoms (∼2.1 μB). As a result of the nature of the couplings (antiferromagnetic vs ferromagnetic) and the magnitude of atomic magnetic moments (∼0.8 μB vs ∼2.1 μB), the PDOS for majority and minority spin electrons are rather similar in ζ_2-GaCr but not for ζ_2-GaFe (see Figure 8). Indeed, in ζ_2-GaFe the DOS for the spin up electrons are mostly occupied whereas for the spin down electrons the DOS are close to half-occupied. This shift between the majority spin states and minority spin states corroborates the total magnetic moment per cell calculated for ζ_2-GaCr (2.529 μB/cell) and ζ_2-GaFe (24.442 μB/cell). A COHP study has also been performed to analyze the interactions between the magnetic atoms, shown in Figure 9. Blue and red have been used to separate the contribution from one spin to the other. The COHP values corresponding to the J_1 and J_2 couplings have been plotted separately for ζ_2-GaCr and ζ_2-GaFe even if they are expected to be similar since the two couplings are identical in the Cr and Fe compounds.

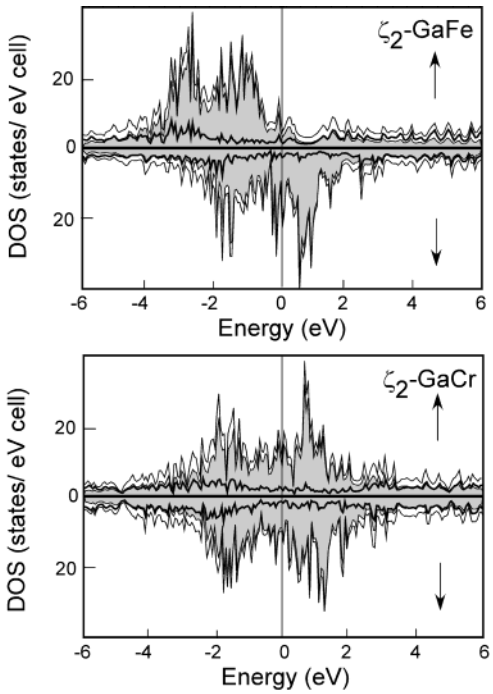

Figure 8. Total density of states (TDOS) and different partial densities of states (PDOS) for the spin-polarized calculations on ζ_2-GaM (M = Cr and Fe).

Variation in the Sign of Exchange with Valence Electron Count. The experimental and theoretical investigation of the isostructural series ζ_2-GaM, M = Cr, Mn, Fe, revealed a systematic change in the sign of the net exchange coupling from antiferromagnetic (AFM) in the nearly half-

(21) Janak, J. F. *Phys. Rev. B* **1977**, *16* (1), 255−262.

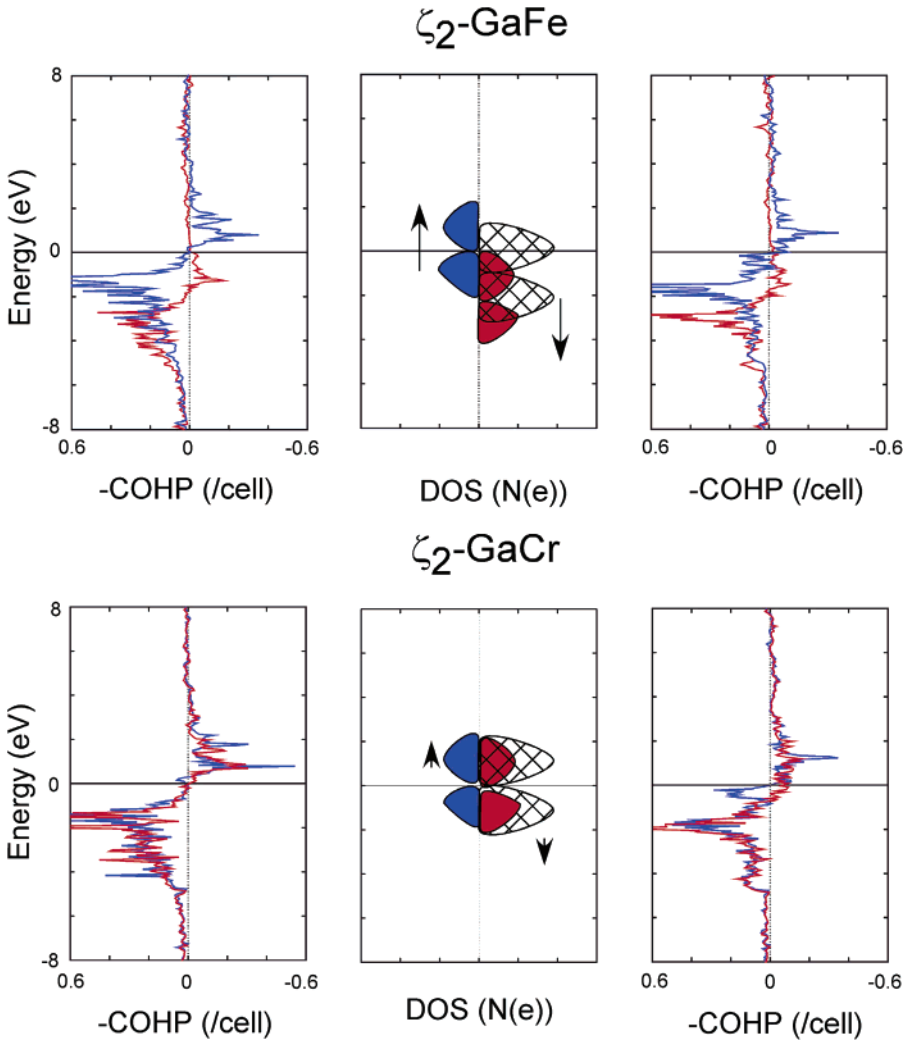

Figure 9. M−M COHP curves for the ζ_2-GaCr and GaFe. A scheme of the TDOS is also presented. The hatched area illustrated the DOS for the non-spin-polarized calculation.

filled d-band case of ζ_2-GaCr to ferromagnetic (FM) in ζ_2-GaFe. A similar sequence is observed in the elements Cr through Fe themselves, although there are structural differences. A theoretical study of the relationship between the sign of the exchange interaction between two magnetic impurities in a metallic matrix and the number of valence electrons was examined four decades ago by Alexander and Anderson, who demonstrated AFM coupling near the half-filled occupancies and FM coupling near the extremes (nearly empty or full).[22] In this model, the occurrence of magnetic moments at the impurity sites originated from a Hubbard-like on-site repulsion from two electrons occupying the same one-electron orbital. This repulsion is further modified by the attractive intra-atomic exchange energy resulting from degenerate orbitals occupied by electrons with identical spins.

The converged results from the TB-LMTO calculations on ζ_2-GaM using LSDA reproduce the observed experimental trend in magnetic character, but still cannot provide additional insights into the nature of these interactions. To attempt this, we have carried out simplified (noniterative), tight-binding,

Scheme 1

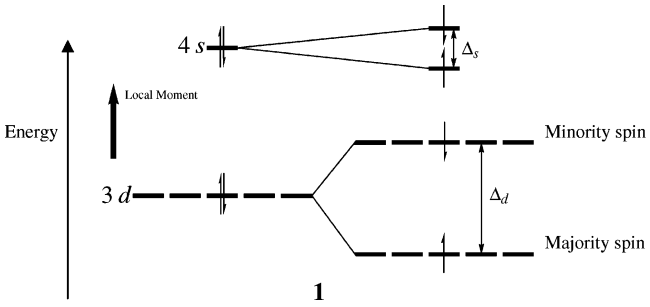

1

one-electron calculations designed to mimic the effects of the exchange splitting of the up-spin and down-spin electrons on M_{12} icosahedra. In this model, the energies of the one-electron orbitals, which can hold two electrons, are split into a lower energy, majority spin orbital (A) and a higher energy, minority spin orbital (B; see Scheme 1).[23] The energy difference between these two spin-orbitals is a measure of the intraatomic exchange energy. Then, tight-binding calculations are carried out for each spin manifold: in the case

(22) Alexander, S.; Anderson, P. W. *Phys. Rev. A* **1964**, *133* (6A), 1594−1603.

(23) Pettifor, D. *Structure and Bonding in Molecules and Solids*; Oxford: London, 1994.

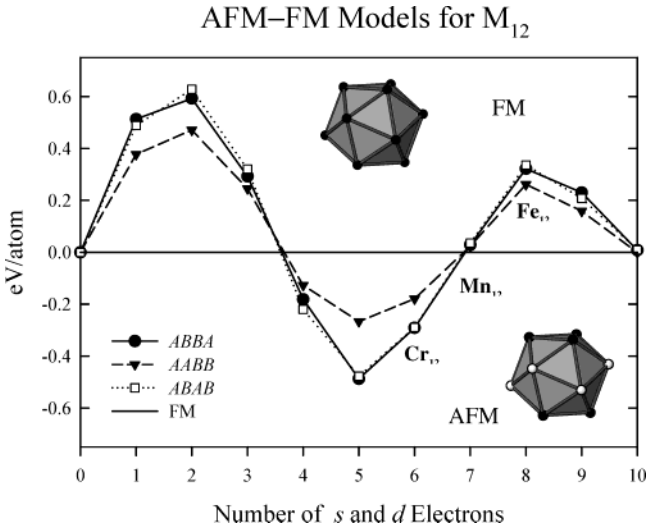

Figure 10. Energy difference curves between AFM and FM coupled models of magnetic exchange in M_{12} icosahedra as a function of valence electron count. Positive energies favor the FM model, and negative energies favor the AFM models. Valence electron counts for Cr_{12}, Mn_{12}, and Fe_{12} icosahedra are noted.

of FM coupling, one for the majority spins, another for the minority spins; in the cases of AFM coupling, just one calculation is needed, but it behaves like a heteroatomic (bimetallic) calculation.[23] For this calculation, we utilized the Wolfsberg−Helmholz approximation[24] for the resonance integrals and valence d and s atomic orbitals for Fe. The splittings of the d and s orbitals were those obtained from the TB-LMTO calculations within the LSDA (1.60 eV for 3d and 0.50 eV for 4s). It is important to realize that this model calculation is not suited to compare nonmagnetic with magnetic (i.e., spin-polarized) structures, but given the presence of local magnetic moments at M sites, this model is designed to probe the relative energies of different magnetic structures based on the same on-site, exchange-correlation potential for the valence electrons.

The results from these simple calculations on a M_{12} icosahedron are illustrated in the energy difference curves in Figure 10. These curves compare the total energies for three different AFM models against the FM model; all curves between 0 and 10 sd electrons per M atom show fourth-behavior, which is indicative of homonuclear versus heteronuclear interactions in a binary system.[25] (Quantitatively, the results in Figure 10 are valid just near M = Mn and Fe. However, the qualitative features of the curve are general for all band fillings and are shown to emphasize the fourth-moment behavior.) Near the half-filled band cases, AFM coupling is strongly preferred, and nearer the extreme cases, FM coupling is preferred (in a one-electron study of binary alloys (MN), heteronuclear M−N interactions are preferred near the half-filled band and homonuclear M−M and N−N interactions are preferred near the extremes). This simple calculation nicely reproduces the results of the TB-LMTO-LSDA calculations on ζ_2-GaM, M = Cr, Mn, Fe. Furthermore, among the AFM cases, there are three distinct models (ABBA, ABAB, and AABB), which differ in the numbers of nearest neighbor FM ("homonuclear") and AFM ("heteronuclear") couplings. AFM models ABBA and ABAB have 12 FM and 18 AFM couplings; AABB has 18 FM and 12 AFM couplings, and these are indicative in the curves. The two AFM models with more nearest neighbor AFM couplings are most preferred near the half-filled band. Indeed, the case of ζ_2-GaMn represents an interesting magnetic situation: the energy differences between the different FM and AFM models are nearly zero.

Thus, this simple calculation strongly suggests that the trend in AFM versus FM coupling in itinerant systems behaves as a fourth-moment problem of the density of states. From a single band calculation using the Hubbard model, which explicitly includes the competition between resonance integrals (electron delocalization) and intra-atomic Coulomb repulsion (localization), the tendency toward ferromagnetism is stronger above the half-filled band than below it.[26] Both of these conclusions are consistent with the current statements of Dronskowski et al.,[19] and further experimental and empirical study of magnetic systems will help us achieve some chemical guidelines to find interesting magnetic systems.

Summary

Spin-polarized calculations predict that for ζ_2-GaM (M = Cr, Mn, or Fe) from Cr to Fe, there is a change in the magnetic behavior from a weakly antiferromagnetic compound to a ferromagnetic one. Analyses of their electronic structures are consistent with Dronskowski's studies, which show that a driving force for antiferromagnetism or ferromagnetism lies in the local nonbonding or antibonding character of the states around the Fermi level. Magnetic measurements confirm ferromagnetic behavior for ζ_2-GaFe and show a weak paramagnetic response for ζ_2-GaCr. Syntheses are currently in progress by mixing Cr and Fe with the same ζ_2-GaM structure type to see how the magnetic behavior compares to this hypothesis.

Acknowledgment. The Ames Laboratory is operated for the U.S. Department of Energy by Iowa State University under Contract W-7405-ENG-82. This work was supported by the Office of Basic Energy Sciences, Materials Sciences Division of the U.S. Department of Energy. Also, a part of this work was supported by NSF Grants DMR-99-81766 and DMR-02-41092. The authors are grateful to Warren Straszheim of the Materials Analysis Research Laboratory of Iowa State University for running energy-dispersive X-ray spectroscopy measurements on our samples.

Supporting Information Available: CIF files giving positional and thermal parameters and bond angles for ζ_2-GaCr and ζ_2-GaFe. This material is available free of charge via the Internet at http://pubs.acs.org.

IC035419F

(24) Burdett, J. K. *Molecular Shapes*; Wiley: New York, 1978.
(25) Burdett, J. K. *Chemical Bonding in Solids*; Wiley: New York, 1990.
(26) Pastor, G. M.; Hirsch, R.; Mühlschlagel, B. *Phys. Rev. B* **1996**, *B53* (15), 10382−96.